



# High birefringence photonic crystal fiber for glucose sensing

Muhamed A. Sewidan<sup>1</sup> · Muhammad A. Othman<sup>1</sup> · Mohamed A. Swillam<sup>1</sup>

Received: 6 June 2023 / Accepted: 30 August 2023 / Published online: 21 October 2023  
© The Author(s) 2023

## Abstract

This paper focuses on designing a simple photonic crystal fiber (PCF) biosensor. The proposed glucose sensor is modelled by Lumerical software using the finite element method. To evaluate the efficiency of this model, different sensing properties such as birefringence, coupling length, and relative sensitivity are calculated at different air-filling fractions. The principle of this PCF is to detect the variations in the refractive index of the different concentration glucose solutions. The analyte will be injected into an elliptical channel surrounded by two rings of air holes in a hexagonal shape. Numerical simulations show that increasing the air-filling fraction yields high performance and more light confinement. At the air-filling fraction of 0.45, the maximum birefringence and relative sensitivity were  $4.01 \times 10^{-3}$  and 91%, respectively. Also, the coupling length reaches a minimum of 162.09  $\mu\text{m}$ .

**Keywords** Photonic crystal · Optical fiber · Biosensors · Birefringence · Glucose sensing

## 1 Introduction

Diabetes is considered one of the most spread chronic diseases all over the globe (W. Organization 2016). By definition, it is a metabolic disorder in which the sugar level in the blood is high for a long time (W. Organization 2016). Based on the World Health Organization (WHO) surveys, more than 463 million people had diabetes worldwide in 2019 (W. Organization 2016). The later symptoms of diabetes can lead to several complications among them increased thirst, stroke, blindness, diabetic ketoacidosis, and eventually death (Yan et al. 2023). Diabetes is caused because either the pancreas is improperly secreting insulin, or the body cells are not responding efficiently to the insulin (Wang et al. 2022). In the meantime, there is no certain cure for diabetes. Nevertheless, diabetes is better dealt with by monitoring the glucose level in the blood. Therefore, it is of great interest for researchers to develop glucose sensors with high sensitivities, small footprints, and commercial prices.

---

✉ Mohamed A. Swillam  
m.swillam@aucegypt.edu

<sup>1</sup> Department of Physics, School of Science and Engineering, The American University in Cairo, New Cairo 11835, Egypt

Compact optical sensors based on different platforms such as photonic crystal fibers (PCFs) (Azad et al. 2022; Kaur et al. 2022; Mumtaz et al. 2023; Zhao et al. 2022), silicon photonic (Fouad et al. 2020; Mehaney et al. 2021), plasmonic (Hassanen et al. 2020; Wang et al. 2021b) were developed with different functioning mechanisms including directional couplers (Uddin et al. 2021), ring resonators (Tan et al. 2021b), Mach–Zehnder (Amin et al. 2021) and multi-mode interferometers (Wang et al. 2021a). Photonic crystal fiber sensors have gained a lot of attention in the recent years owing to the strong light-matter interaction in line and cavity defects in their photonic crystal structures, and their fabrication maturity (silica fibers). The air holes forming the photonic crystal structure in PCFs can be infiltrated with analytes to monitor the interaction of electromagnetic radiation with the analyte material and its impact on different parameters such as coupling length, birefringence and relative sensitivity. Different applications of PCF sensors were reported such as biosensors (Meshginqalam and Barvestani 2022; Sarker et al. 2021), temperature (Dhara and Singh 2021; Rabbi et al. 2021), pressure (Gowda et al. 2023; Yang et al. 2021), gas and liquid sensors (Eid et al. 2021; Fard et al. 2021; Maida et al. 2021; Sardar et al. 2021). One key characteristic of PCFs is tunable birefringence (Devika et al. 2022). The values of birefringence obtained from PCFs is higher than that of conventional birefringent fiber by an order of  $10^3$  magnitude (Tan et al. 2021a). Also, the obtained birefringence from PCFs is significantly insensitive to temperature (Rajan et al. 2022) which results in operation stability of the sensor at different surrounding temperatures, which makes such sensors highly desirable in different working environments and operation sites. High birefringent PCFs are used in polarization-maintaining fibers for optical fiber sensing (Leon et al. 2021), special lasers (Li et al. 2022) and long-distance communications (Yu et al. 2022). Birefringence occurs when the two orthogonal polarized modes in the fiber travel at different speeds due to an introduced asymmetry in the core region. This asymmetry can be achieved by creating an asymmetric central defect or by changing the shape and the size of the air holes around the fiber's core. So far, numerous PCFs are proposed for diabetes sensing. However, to the best of our knowledge, we hereby report the highest birefringence values for such PCF sensors, owing to the detailed study and optimization of the air-filling fraction.

In this paper, we propose a simple design of PCF that can be used as a glucose sensor. This design is chosen to be as simple as possible for easy fabrication. The sensing principle of this PCF is to monitor the variations in the refractive index of glucose solutions with different concentrations. The performance of this fiber is further investigated by determining some key parameters such as birefringence, relative sensitivity and coupling length. The structure parameters of this fiber are studied to optimize its performance. A comparison between the performance of our model and others from the literature is to given to show the efficiency of our model. Furthermore, we introduce all the technical and experimntal requirements needed for manufacturing and operating the PCF.

## 2 Design and working principle

The proposed glucose-sensing PCF, shown in Fig. 1, has one elliptical channel that is filled with the analyte. This elliptical channel divides the fiber core into two separate cores where the light will propagate in them as shown in the simulations of Fig. 2. Around the core, there is an air-holes hexagonal lattice of two rings. The basic purpose of these air holes is to reduce the mean refractive index of the cladding to maintain a total internal reflection in the core. This design was kept as simple as possible for the ease of manufacture. As increasing the air rings will make the model more complex for fabrication.

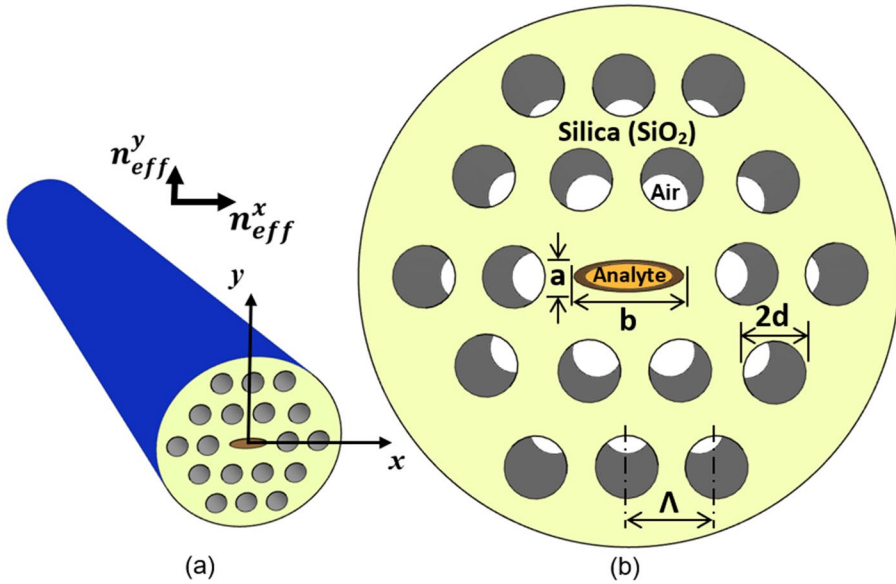
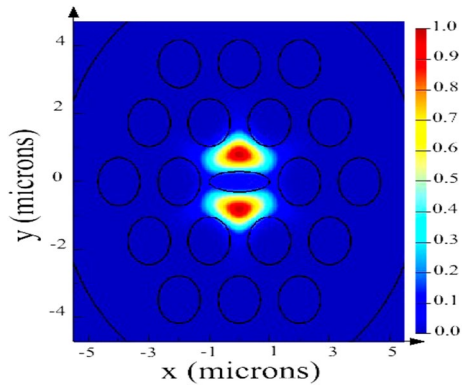


**Fig. 1** **a** Sensing fiber with hollow core for analyte passage and photonic crystal structure surrounding it, **b** The cross-sectional area of the photonic crystal fiber

**Fig. 2** The electric field distribution in the dual-core photonic crystal fiber



The elliptical channel has a minor and major axis of  $a$  and  $b$ , respectively, as shown in Figure 1. In addition, to be used as a channel for infiltration, this channel is used to introduce asymmetry to the propagating mode which gives rise to high birefringence. The cladding consists of two circular air holes rings arranged in a hexagonal shape. The radius of each air hole is  $d$  and the distance between any two adjacent air holes is the pitch, given by  $\Lambda$ . The ratio between air hole radius and the pitch is called the air filling fraction and it has a significant impact on the properties of the PCF. This ratio will be further optimized to investigate for the best possible results.

The fiber diameter is  $6 \mu\text{m}$  and the cladding air holes have a radius  $d = 0.7 \mu\text{m}$  and a pitch  $\Lambda = 2 \mu\text{m}$  ( $d/\Lambda = 0.35$ ). The elliptical air hole has a semi-major axis  $b = 1 \mu\text{m}$

**Table 1** The refractive index of some glucose solutions with different concentrations

Glucose concentration (g/L)	$n_g$
0	1.332305
10	1.333494
20	1.334683
30	1.335872
40	1.337061

and a semi minor axis  $a = 0.3 \mu\text{m}$  ( $a/b = 0.3$ ). For this model, fused silica was chosen to be the sensor's clad material. Fused silica has several positive aspects including being inert with chemicals, having high thermal stability, and can be used in ultraviolet to near-infrared applications (Hasan et al. 2017). The refractive indices values of silica are given using Lumerical's library (Palik 1998).

There are several fabrication techniques that can be used to fabricate this model such as sol-gel casting, stack-and-draw, die casting, and extrusion (Yajima et al. 2013). Circular air holes can be fabricated using sol-gel or stack-and-draw techniques. While the elliptical air holes can be made using die casting (Guiyao et al. 2006) or chemical polymerization method (Zhang et al. 2006). For the elliptical channel infiltration, numerous techniques can be used such as the fusion splicer-based collapsing-cladding air hole (Xiao et al. 2005) or the femtosecond laser-supported technique (Wang et al. 2010). In the first technique, the central hole was infiltrated with some polymer by the capillary action, and then the polymer was cured by a UV lamp, finally the fiber ends were cleaved. For reusing the fiber, it is vital to dispose of all the residuals from previous samples. The cleaning agent has to interact strongly with the sample and gently with the fiber walls. For polar analytes, surface adsorption must be prevented by introducing a hydrophobic silane layer. For nonpolar analytes, the continuous flow of a good cleaning agent can solve this problem.

The refractive index RI of the glucose solutions  $n_g$  is calculated using the following equation (An et al. 2017):

$$n_g = 11.889 \times 10^{-5} \times \text{GC} + 1.332305 \quad (1)$$

Where GC is the concentration of glucose solution (g/L). Table 1 presents the RI of the analytes used in our study.

### 3 Theoretical background

Finite element method (FEM) was used to numerically analyze the PCF model in Lumerical MODE module <https://support.lumerical.com/hc/en-us/articles/1500007184901-Lumerical-Citation-Instruction>. This method can provide us with the comprehensive performance of this PCF. Also, several equations were used to fully characterize the optical properties to investigate the effectiveness of this model. The investigated parameters are birefringence, coupling length, and relative sensitivity.

Birefringence B equals the difference between the two real parts of the effective index of two perpendicular polarization states; x-polarization and y-polarization, its formula is (Isti et al. 2020):

$$B = \left| n_{eff}^x - n_{eff}^y \right| \tag{2}$$

Coupling length  $L_c$  of any fiber gives the exact length where the total optical power between two polarization states is transferred. It can be calculated using the following equation (Mollah et al. 2020):

$$L_c = \frac{\lambda}{\left| n_{eff}^x - n_{eff}^y \right|} \tag{3}$$

In order to investigate the ability of the fiber to detect any analytes, the relative sensitivity  $r$  must be calculated. It is defined as (Eid et al. 2021):

$$r = \frac{n_r}{n_{eff}} f \tag{4}$$

Where  $n_r$  is the refractive index of the used analyte,  $n_{eff}$  is the real part of the effective index of mode and  $f$  is the total power fraction delivered in the core region.

### 4 Results and discussion

Air-filling fraction is a key parameter in PCF as it controls the power delivery and the confinement loss. We used three different values of the air-filling fraction to investigate their influence on the PCF performance parameters such as birefringence. Firstly, we used an air-filling fraction of 0.35, air hole radius = 0.7  $\mu\text{m}$  and pitch = 2  $\mu\text{m}$ .

Figure 3 shows the birefringence of the five glucose concentrations at this air-filling fraction. It is clearly seen that; the highest birefringence values are related to the analyte with the lowest concentration (0 g/L). This can be explained that, increasing the RI of the

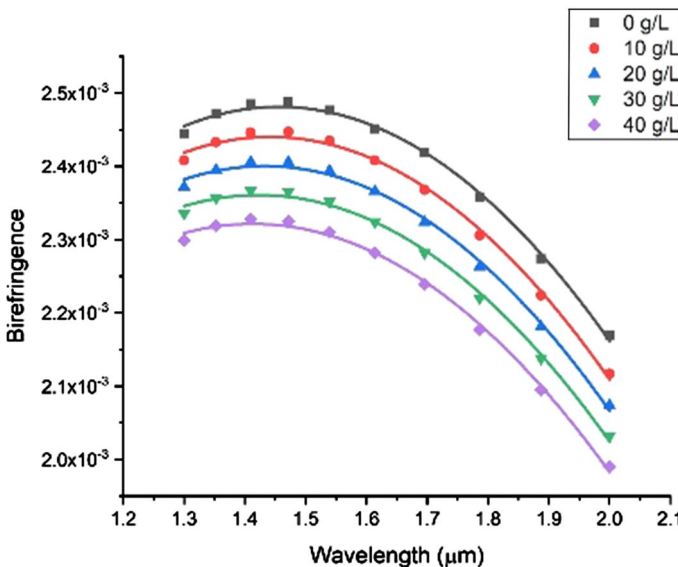
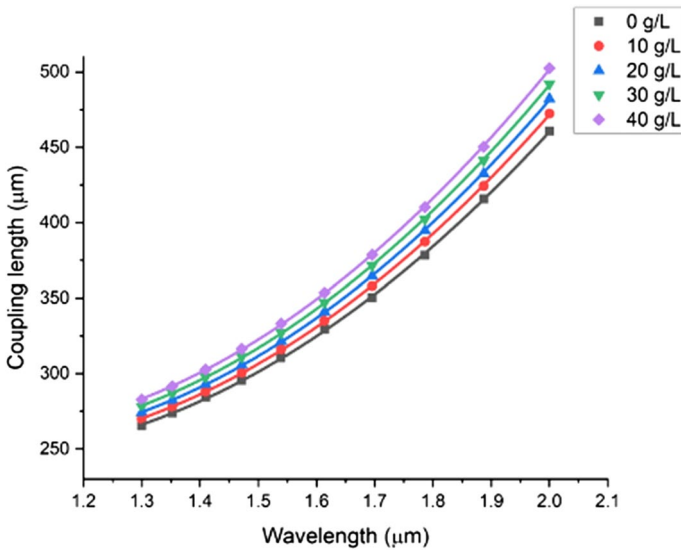


Fig. 3 The relation between the birefringence and wavelength for the air-filling fraction of 0.35



**Fig. 4** The relation between coupling length and wavelength for the air-filling fraction of 0.35

analyte, increased the two cores mean RI. Hence, they have RI nearly equals to the analyte refractive index. Thus, light leaks from the two cores into the elliptical channel and it became a part of the solid core.

Figure 4 represents the coupling length of the different glucose solutions. It is obviously seen that increasing the operating wavelength and the concentration of the glucose solution will increase the coupling length. The relative sensitivity was calculated for all the concentrations at the x-polarization modes. The calculated sensitivities were 84.55%, 84.66%, 84.92%, 84.97%, 85.02% for the concentrations of 0, 10, 20, 30, and 40, respectively. This can be explained that, by increasing the analyte refractive index, the power delivered in the core region increased due to the reduced confinement loss.

Then, we increased the air-filling fraction to 0.40 by increasing the air hole radius to 0.8  $\mu\text{m}$ . Figure 5 shows the birefringence of the different glucose concentrations at this air-filling fraction. This figure shows a significant increase in the birefringence values for all concentrations. Coupling length was also calculated and illustrated in Fig. 6. The values showed a steady increase, especially for high glucose concentration solutions. To complete our investigation about this air-filling fraction, we calculated the relative sensitivity for 0, 10, 20, 30, and 40 concentrations and found them to be 89.11%, 89.21%, 89.31%, 89.41% and 89.51%, respectively.

Finally, the air-filling fraction of 0.45 was used by increasing the air holes radius to 0.9  $\mu\text{m}$ . This was the maximum air-filling fraction to reach as the air holes will overlap at higher fractions. Figure 7 shows the relation between the birefringence and the operating wavelength. The values of birefringence showed a notable increase compared to the birefringence of other air-filling fractions. On the other hand, coupling length, depicted in Fig. 8, showed a significant decrease for this fraction. Relative sensitivity

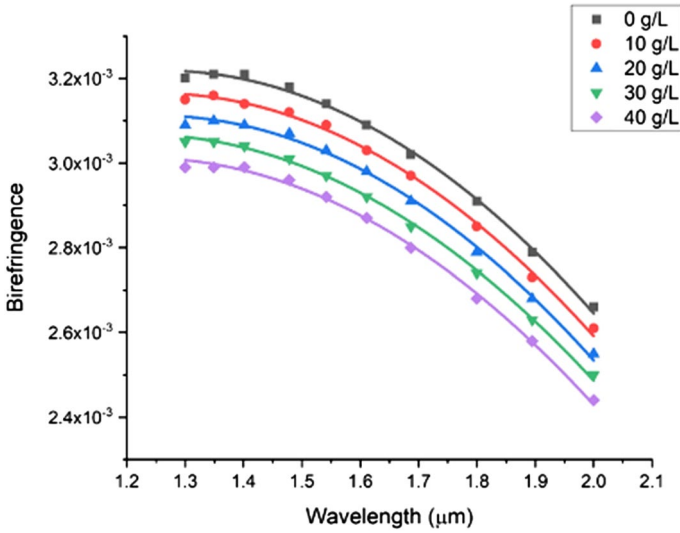


Fig. 5 The relation between birefringence and wavelength for the air-filling fraction of 0.40

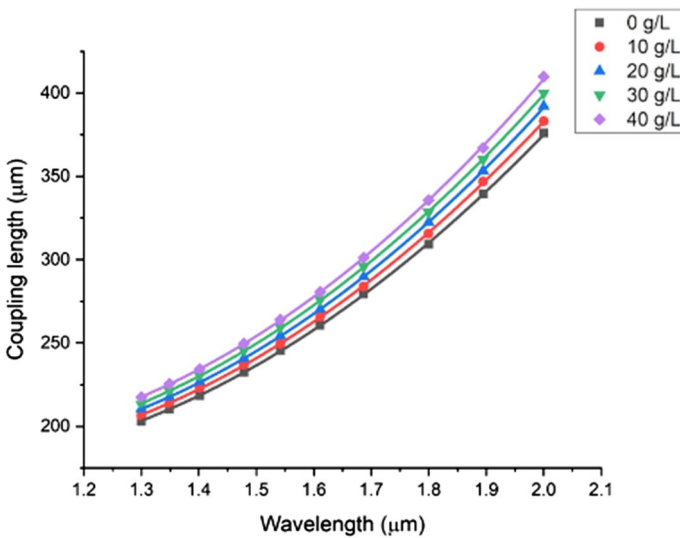


Fig. 6 The relation between coupling length and wavelength for the air-filling fraction of 0.40

was determined for the different concentrations and found to be 89.93%, 90.02%, 90.12%, 90.20% and 91.00%, respectively. Increasing the air-filling fraction increased the birefringence from nearly  $2.5 \times 10^{-3}$  to  $4 \times 10^{-3}$ . Table 2 represents a comparison between the calculated birefringence and other values in previous literature.

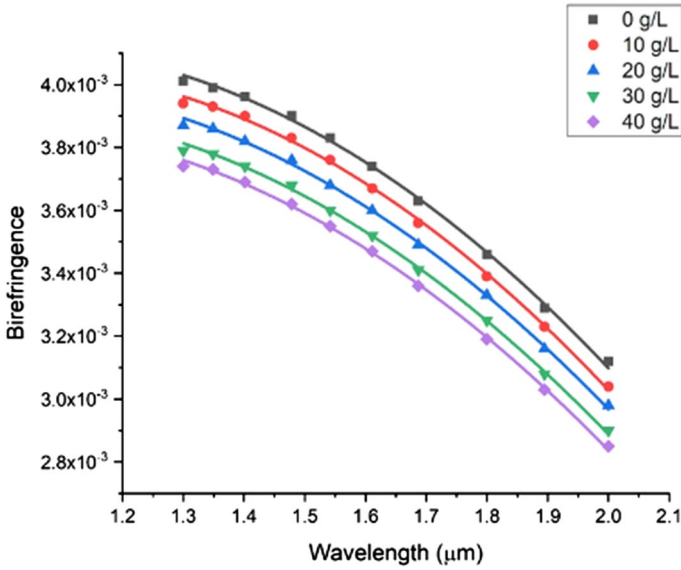


Fig. 7 The relation between birefringence and wavelength for the air-filling fraction of 0.45

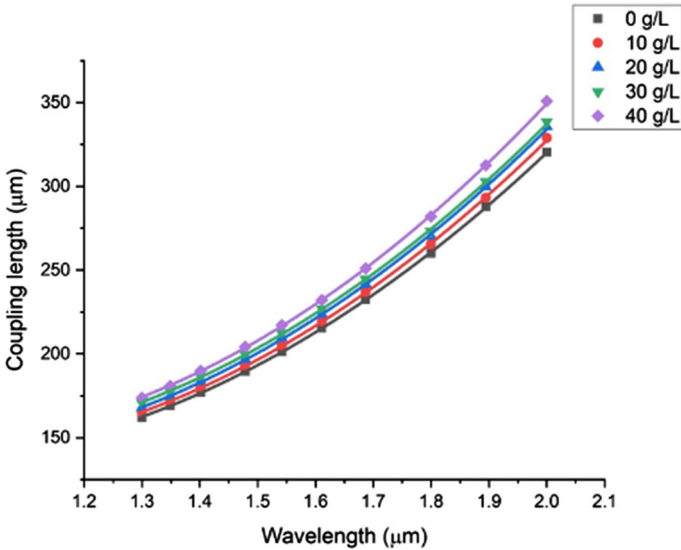


Fig. 8 The relation between coupling length and wavelength for the air-filling fraction of 0.40

In conclusion, our proposed model introduces a high birefringence for glucose sensing. Also, we found that increasing the air-filling fraction can increase the birefringence and the relative sensitivity, and decrease the coupling length significantly.



**Table 2** A comparison between the previous mentioned birefringence values and our calculated value.

Model	Birefringence
Yousufali et al. (2021)	$(3-7) \times 10^{-5}$
An et al. (2017)	$(1-5) \times 10^{-5}$
Ademgil and Haxha (2016)	$8.5 \times 10^{-4}$
Leon et al. (2021)	$2.7 \times 10^{-3}$
Asaduzzaman et al. (2022)	$2.6 \times 10^{-3}$
Kumar et al. (2021)	$2.0 \times 10^{-4}$
Vijayalakshmi et al. (2021)	$1.4 \times 10^{-6}$
Our model	$(2-4) \times 10^{-3}$

## 5 Conclusion

In this study, we suggested a simple design of photonic crystal fiber for diabetes sensing. The detection principle is based on the change in refractive index of the blood sample. In order to enhance the sensor performance, the sensor performance was studied at different air-filling fractions. At the air-filling fraction 0.45, the sensor showed the highest birefringence of  $4.01 \times 10^{-3}$ , relative sensitivity of 91%, and the lowest value of coupling length of 162.09  $\mu\text{m}$ . Due to the features such as simple design, portability, easy detection process, and environmental compatibility, we think that the suggested PCF sensor can be used as a diabetes sensor in the near future.

**Author contributions** MAS conceived the basic idea and validated the concept of operation through analytical and numerical modelling, designed and optimized the device through computer-aided simulations, performed simulations, analyzed the results and wrote the paper. MAO and MAS supervised the entire project. All the authors contributed to the general discussion and revision of the manuscript.

**Funding** Open access funding provided by The Science, Technology & Innovation Funding Authority (STDF) in cooperation with The Egyptian Knowledge Bank (EKB). This work is not funded by any research funds.

**Data availability** The datasets of this work is available on demand from the authors under valid scientific request.

## Declarations

**Conflict of interest** The authors declare that the research was conducted in the absence of any commercial or financial relationships that could be construed as a potential conflict of interest.

**Open Access** This article is licensed under a Creative Commons Attribution 4.0 International License, which permits use, sharing, adaptation, distribution and reproduction in any medium or format, as long as you give appropriate credit to the original author(s) and the source, provide a link to the Creative Commons licence, and indicate if changes were made. The images or other third party material in this article are included in the article's Creative Commons licence, unless indicated otherwise in a credit line to the material. If material is not included in the article's Creative Commons licence and your intended use is not permitted by statutory regulation or exceeds the permitted use, you will need to obtain permission directly from the copyright holder. To view a copy of this licence, visit <http://creativecommons.org/licenses/by/4.0/>.

## References

- Ademgil, H., Haxha, S.: Highly birefringent nonlinear PCF for optical sensing of analytes in aqueous solutions. *Opt. Int. J. Light Electron Opt.* **127**(16), 6653–6660 (2016)
- Amin, R., Maiti, R., Gui, Y., Suer, C., Miscuglio, M., Heidari, E., Khurgin, J.B., Chen, R.T., Dalir, H., Sorger, V.J.: Heterogeneously integrated ITO plasmonic Mach-Zehnder interferometric modulator on SOI. *Sci. Rep.* **11**(1), 1–12 (2021)
- An, G., Li, S., An, Y., Wang, H., Zhang, X.: Glucose sensor realized with photonic crystal fiber-based Sagnac interferometer. *Opt. Commun.* **405**, 143–146 (2017)
- Asaduzzaman, S., Rehana, H., Chakma, R., Faragallah, O.S., El-Sayed, H.S., Eid, M., Rashed, A.N.Z.: Hexa-sectored square photonic crystal fiber for blood serum and plasma sensing with ultralow confinement loss. *Appl. Phys. A* **128**(6), 1–11 (2022)
- Azad, S., Khosravi, M., Nikzad, A., Mishra, S.K.: A novel contemporary molecular imprinting technique for non-enzymatic selective glucose detection. *Opt. Laser Technol.* **148**, 107786 (2022)
- Devika, V., Mani Rajan, M.S., Sharma, M.: Diamond core PET-PCF for supercontinuum generation using meager power with very low birefringence. *Opt. Quantum Electron.* **54**(12), 858 (2022)
- Dhara, P., Singh, V.K.: Investigation of rectangular solid-core photonic crystal fiber as temperature sensor. *Microsyst. Technol.* **27**(1), 127–132 (2021)
- Eid, M.M., Habib, M.A., Anower, M.S., Rashed, A.N.Z.: Highly sensitive nonlinear photonic crystal fiber based sensor for chemical sensing applications. *Microsyst. Technol.* **27**(3), 1007–1014 (2021)
- Fard, A.M., Sarraf, M.J., Khatib, F.: Design and optimization of index guiding photonic crystal fiber-based gas sensor. *Optik* **232**, 166448 (2021)
- Fouad, N., Badr, M., Fedawy, M., Swillam, M.: Shallow silicon sub-wavelength grating waveguide for electro-optical modulation. *Opt. Commun.* **474**, 126098 (2020)
- Gowda, R.B., Sharan, P., Saara, K.: 1-dimensional silicon photonic crystal pressure sensor for the measurement of low pressure. *Results Opt.* **10**, 100352 (2023)
- Guiyao, Z., Zhiyun, H., Shuguang, L., Lantian, H.: Fabrication of glass photonic crystal fibers with a die-cast process. *Appl. Opt.* **45**(18), 4433–4436 (2006)
- Hasan, M.R., Akter, S., Ahmed, K., Abbott, D.: Plasmonic refractive index sensor employing niobium nanofilm on photonic crystal fiber. *IEEE Photon. Technol. Lett.* **30**(4), 315–318 (2017)
- Hassanen, A.M., Akef, S., Swillam, M.A.: Performance enhancement of a thermo-photovoltaic (TH-PV) hybrid system using a plasmonic IR absorber. In: Freundlich, A., Sugiyama, M., Collin, S. (eds.) *Physics, simulation, and photonic engineering of photovoltaic devices IX*, vol. 11275, p. 1127519. International Society for Optics and Photonics, Bellingham (2020)
- <https://support.lumerical.com/hc/en-us/articles/1500007184901-Lumerical-Citation-Instruction>
- Istı, M.I.A., Talukder, H., Islam, S.R., Nuzhat, S., Hosen, A.S., Cho, G.H., Biswas, S.K.: Asymmetrical D-channel photonic crystal fiber-based plasmonic sensor using the wavelength interrogation and lower birefringence peak method. *Results Phys* **19**, 103372 (2020)
- Kaur, B., Kumar, S., Kaushik, B.K.: Advances in photonic crystal fiber: sensing and supercontinuum generation applications. *Opt. Fiber Technol.* **72**, 102982 (2022)
- Kumar, A., Verma, P., Jindal, P.: Decagonal solid core PCF based refractive index sensor for blood cells detection in terahertz regime. *Opt. Quantum Electron.* **53**(4), 1–13 (2021)
- Leon, M.J.B.M., Abedin, S., Kabir, M.A.: A photonic crystal fiber for liquid sensing application with high sensitivity, birefringence and low confinement loss. *Sens. Int.* **2**, 100061 (2021)
- Li, T., Yan, F., Han, W., Feng, T., Guo, Y., Qin, Q., Bai, Z., Cheng, D., Yang, D.: A multi-wavelength thulium-doped fiber laser using a photonic crystal fiber-based sagnac loop. *IEEE Photon. J.* **14**(1), 1–7 (2022)
- Maidi, A.M.I., Abas, P.E., Petra, P.I., Kaijage, S., Zou, N., Begum, F.: Theoretical considerations of photonic crystal fiber with all uniform-sized air holes for liquid sensing. *Photonics* **8**(7), 249 (2021)
- Mehaney, A., Abadla, M.M., Elsayed, H.A.: 1D porous silicon photonic crystals comprising Tamm/Fano resonance as high performing optical sensors. *J. Mol. Liq.* **322**, 114978 (2021)
- Meshginqalam, B., Barvestani, J.: High performance surface plasmon resonance-based photonic crystal fiber biosensor for cancer cells detection. *Euro. Phys. J. Plus* **137**(4), 417 (2022)
- Mollah, M.A., Yousufali, M., Ankan, I.M., Rahman, M.M., Sarker, H., Chakrabarti, K.: Twin core photonic crystal fiber refractive index sensor for early detection of blood cancer. *Sens. Bio-Sens. Res.* **29**, 100344 (2020)
- Mumtaz, F., Yaseen, G., Roman, M., Abbas, L.G., Ashraf, M.A., Fiaz, M.A., Dai, Y.: Numerical analysis of the highly non-linear and ultra-sensitive modified core of a photonic crystal fiber sensor for detection of liquid analytes. *JOSA B* **40**(1), 142–150 (2023)
- Organization, W.: Global report on diabetes. <http://www.who.int/diabetes/global-report/en/>. (2016)

- Palik, E.D. (ed.): Handbook of optical constants of solids, vol. 3. Academic press, London (1998)
- Rabbi, F., Rahman, M.T., Khaleque, A., Rahman, M.M.: Theoretical analysis of Sagnac Interferometer based highly sensitive temperature sensor on photonic crystal fiber. *Sens. Bio-Sens. Res.* **31**, 100396 (2021)
- Rajan, M.S.M.: Photonic crystal fibers for various sensing applications. In: Mallakpour, S., HussainIndustrial, C.M. (eds.) Applications of nanocrystals, pp. 3–21. Elsevier, Amsterdam (2022)
- Sardar, M.R., Faisal, M., Ahmed, K.: Simple hollow Core photonic crystal Fiber for monitoring carbon dioxide gas with very high accuracy. *Sens. Bio-Sens. Res.* **31**, 100401 (2021)
- Sarker, H., Faisal, M., Mollah, M.A.: Slotted photonic crystal fiber-based plasmonic biosensor. *Appl. Opt.* **60**(2), 358–366 (2021)
- Tan, H., Sima, C., Deng, B., Zhang, X., Chen, G., Yu, Q., Xu, J., Lian, Z., Liu, D.: Design and analysis of ultra-wideband highly-birefringent bragg layered photonic bandgap fiber with concave-index cladding. *IEEE Photon. J.* **13**(3), 1–10 (2021)
- Tan, M., Xu, X., Wu, J., Nguyen, T.G., Chu, S.T., Little, B.E., Mitchell, A., Morandotti, R., Moss, D.J.: Orthogonally polarized RF optical single sideband generation with integrated ring resonators. *J. Semiconduct.* **42**(4), 041305 (2021)
- Uddin, M.F., Hafez, M.G., Hammouch, Z., Rezaaddeh, H., Baleanu, D.: Traveling wave with beta derivative spatial-temporal evolution for describing the nonlinear directional couplers with metamaterials via two distinct methods. *Alex. Eng. J.* **60**(1), 1055–1065 (2021)
- Vijayalakshmi, D., Manimegalai, C.T., Ayyanar, N., Vigneswaran, D., Kalimuthu, K.: Detection of blood glucose with hemoglobin content using compact photonic crystal fiber. *IEEE Trans. NanoBiosci.* **20**(4), 436–443 (2021)
- Wang, X., Gao, M., Wang, Y., Zhang, Y.: The progress of pluripotent stem cell-derived pancreatic  $\beta$ -cells regeneration for diabetic therapy. *Front. Endocrinol.* **13**, 927324 (2022)
- Wang, Y., Liao, C.R., Wang, D.N.: Femtosecond laser-assisted selective infiltration of microstructured optical fibers. *Opt. express* **18**(17), 18056–18060 (2010)
- Wang, Z., Yao, C., Zhang, Y., Su, Y.: Compact silicon three-mode multiplexer by refractive-index manipulation on a multi-mode interferometer. *Opt. Express* **29**(9), 13899–13907 (2021)
- Wang, Y., Zhao, C., Wang, J., Luo, X., Xie, L., Zhan, S., Kim, J., Wang, X., Liu, X., Ying, Y.: Wearable plasmonic-metasurface sensor for noninvasive and universal molecular fingerprint detection on biointerfaces. *Sci. Adv.* **7**(4), eabe4553 (2021)
- Xiao, L., Jin, W., Demokan, M.S., Ho, H.L., Hoo, Y.L., Zhao, C.: Fabrication of selective injection microstructured optical fibers with a conventional fusion splicer. *Opt. Express* **13**(22), 9014–9022 (2005)
- Yajima, T., Yamamoto, J., Ishii, F., Hirooka, T., Yoshida, M., Nakazawa, M.: Low-loss photonic crystal fiber fabricated by a slurry casting method. *Opt. express* **21**(25), 30500–30506 (2013)
- Yan, C.L., Zhang, Z.H., Ma, L.Q., Xu, X.Y., Azhar, M., Huang, X., Shi, J.X., Li, J.: Veratrilla baillonii Franch alleviate the symptoms of diabetes in type 2 diabetic rats induced by high-fat diet and streptozotocin. *Food Sci. Hum. Wellness* (2023). <https://doi.org/10.26599/FSHW.2022.9250116>
- Yang, X., Li, Y., Zhang, S., Wang, S., Wu, S.: Comparison of fiber-based gas pressure sensors using hollow-core photonic crystal fibers. *IEEE Photon. J.* **13**(2), 1–9 (2021)
- Yousufali, M.d., Mollah Aslam, M.d., Ahmed, K.: Multimode interference-based photonic crystal fiber glucose sensor. *Plasmonics* **16**(3), 811–818 (2021)
- Yu, Y., Lian, Y., Hu, Q., Xie, L., Ding, J., Wang, Y., Lu, Z.: Design of PCF supporting 86 OAM modes with high mode quality and low nonlinear coefficient. *Photonics* **9**(4), 266 (2022)
- Zhang, Y., Li, K., Wang, L., Ren, L., Zhao, W., Miao, R., Large, M.C., Van Eijkelenborg, M.A.: Casting preforms for microstructured polymer optical fibre fabrication. *Opt. express* **14**(12), 5541–5547 (2006)
- Zhao, Q., Liu, J., Yang, H., Liu, H., Zeng, G., Huang, B., Jia, J.: Double U-groove temperature and refractive index photonic crystal fiber sensor based on surface plasmon resonance. *Appl. Opt.* **61**(24), 7225–7230 (2022)